Solar Energy Materials & Solar Cells 94 (2010) 2238–2243

Contents lists available at ScienceDirect

Solar Energy Materials & Solar Cells

journal homepage: www.elsevier.com/locate/solmat

Formation and photoluminescence of Si quantum dots in SiO_2/Si_3N_4 hybrid matrix for all-Si tandem solar cells

D. Di *, I. Perez-Wurfl, G. Conibeer, M.A. Green

ARC Photovoltaics Centre of Excellence, University of New South Wales, Sydney, NSW 2052, Australia

ARTICLE INFO

Article history:
Received 18 July 2010
Accepted 19 July 2010
Available online 13 August 2010

Keywords:
Silicon quantum dots
Nanocrystal growth
Tandem solar cells
Photoluminescence

ABSTRACT

In this work, Si quantum dots in SiO_2/Si_3N_4 hybrid matrix on quartz substrates were synthesized by magnetron sputtering of alternating silicon rich oxide and Si_3N_4 layers followed by different post-deposition anneals. XRD results indicate that the average dimension of the Si nanocrystals varies from 1.6 to 5.2 nm. The size and crystallization of the Si nanocrystals are dependent on a number of factors, including the annealing method, the SRO thickness and the Si_3N_4 barrier thickness, as evidenced in XRD and Raman measurements. In particular, thicker Si_3N_4 barrier layers seem to be able to suppress the growth of Si nanocrystals more effectively. PL measurements suggest the apparent bandgap of the samples investigated in this work is in the range 1.12–1.67 eV, which demonstrates the effect of quantum confinement. More interestingly, analysis of the PL data using the modified EMA equations clearly suggests that the PL peak energy not only depends on the size of the nanocrystals but also gets affected by other details in nanocrystal growth. A tentative core–shell model is constructed to illustrate our explanation. These findings offer a preliminary understanding of the nanocrystal growth and radiative recombination processes in this newly synthesized material for photovoltaic applications.

1. Introduction

The concept of a tandem solar cell has been well developed as a method of improving solar cell efficiency. In a tandem cell, solar cells of different bandgaps are stacked on top of one another. The cell with the highest bandgap is placed on the very top, while the cell with the lowest bandgap is positioned at the bottom of the tandem stack. Each cell absorbs the light it can most effectively convert, with the rest passing through to the underlying cells [1].

An all-Si tandem solar cell makes use of inexpensive silicon thin-film technology in combination with a high efficiency multi-bandgap approach. It takes the advantage of quantum confinement effects in silicon. When silicon is made very thin (in the order of a few nanometers) in one or more dimensions, quantum confinement causes its effective bandgap to increase. The strongest effect is obtained when silicon is confined in 3D (i.e., quantum dots). If the quantum dots are close to each other, carriers can tunnel between them to form quantum dot superlattices, which can be used as the higher bandgap cells in a tandem stack (Fig. 1(a)) [2].

A simple approach to make quantum dot superlattices has been described by Zacharias et al. [4]. The bandgap of silicon thin-films generated in this way can be varied by varying the size of the quantum dots. This effect has been supported by photoluminescence (PL) measurements [1].

As an important step towards the realization of silicon-based tandem solar cells using silicon quantum dots embedded in a dielectric matrix, we have fabricated single junction Si quantum dot solar cells with open-circuit voltage exceeding 400 mV [3,5]. This was based on Si nanocrystals embedded in a SiO_2 matrix. However, the output current of the cell is strongly limited by the material's high resistivity. One approach of improvement is to replace the SiO_2 tunnelling barriers ($E_g \sim 9$ eV) with a lower bandgap material such as Si_3N_4 ($E_g \sim 5$ eV) (Fig. 1(c)). In addition, Si_3N_4 acts as a better diffusion barrier compared to SiO_2. It restricts the displacement of silicon atoms as well as dopant atoms under high processing temperatures. Therefore, we propose exploring a new type of nanostructured photovoltaic material based on silicon quantum dots embedded in SiO_2/Si_3N_4 hybrid matrix. Although the electrical and photovoltaic properties are of primary interest when the intended application is concerned, other material information such as the Si quantum dot size, the process of nanocrystal formation and the mechanisms of photoluminescence are also important for the development and understanding of the photovoltaic device. To investigate these matters, a series of experimentations have been carried out and are described in the following sections.

2. Experimental

Alternating layers of silicon nitride (Si_3N_4) followed by silicon-rich oxide (SRO) were deposited on quartz substrates by

* Corresponding author. Tel.: +61 2 9385 6782; fax: +61 2 9385 5104.
E-mail addresses: dawei.di@unsw.edu.au, didawei1412@hotmail.com (D. Di).

0927-0248/$ - see front matter © 2010 Elsevier B.V. All rights reserved.
doi:10.1016/j.solmat.2010.07.018

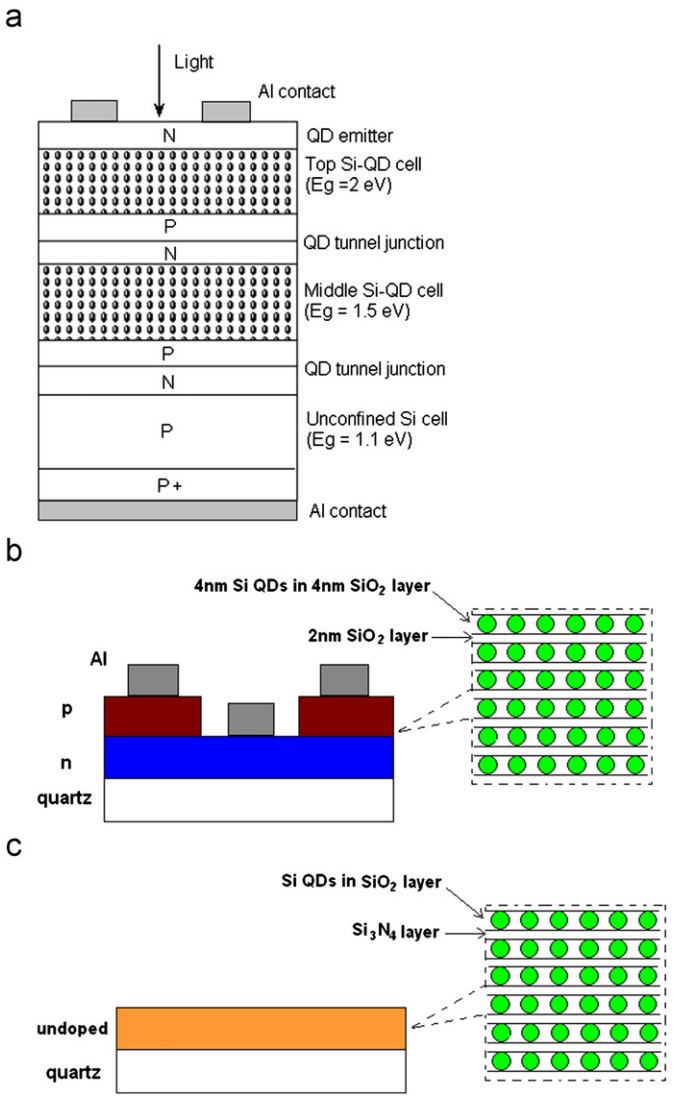

Fig. 1. (a) An all-Si quantum dot superlattice tandem solar cell [2], (b) a single junction Si QD solar cell with demonstrated voltage of more than 400 mV [3] and (c) the material system investigated in this work.

magnetron sputtering of Si_3N_4, intrinsic Si and SiO_2 targets using a computer-controlled AJA ATC-2200 sputtering system. The volume ratio between sputtered Si and SiO_2 was 1:1 as determined by a built-in deposition rate monitor. Prior to sputtering, the chamber of the sputtering system was evacuated to a pressure of $\sim 5\times10^{-7}$ Torr; subsequently the chamber was filled with Ar gas to a working pressure of 1.5 mTorr. The Argon flow was maintained at 15 sccm during the entire deposition process. To demonstrate the size dependence of quantum confinement effect and other material properties, samples were designed to have three different Si_3N_4 layer thicknesses, 1, 2 and 4 nm. Similarly, the intended SRO thicknesses were 2.5, 4 and 5.5 nm. The total thickness of each thin-film specimen was made to be approximately 200 nm, excluding the thickness of the quartz substrate (1 mm). Control of deposition thicknesses was realized through the deposition rate monitor. The intended device structure is illustrated in Fig. 1(c).

After the deposition process, the samples were annealed in a high temperature ambient to facilitate Si QD growth. In this work, three annealing methods are compared. The first method was to process the samples in a rapid thermal anneal (RTA) furnace at 1100 °C for 40 s. The second method was to anneal the samples in a conventional N_2 purged tube furnace. The temperature of the furnace was increased from 600 to 1100 °C over 38 min. As soon as the furnace reaches 1100 °C, it was ramped down back to 600 °C in about 90 min ("Furnace Short"). The third method was to anneal the samples in the same furnace as of method two, but the durations for the samples being kept in a 1100 °C ambient were 30 min, followed by a 90 min ramp-down ("Furnace Long").

The crystalline properties of the samples were studied by glancing angle incidence X-ray diffraction (GI-XRD) (Phillips X'pert Pro) using Cu $K\alpha$ radiation ($\lambda=0.154$ nm), operating at a voltage of 45 kV and a current of 40 mA. The primary optics was defined by using a 1/16° divergent slit in front of a parabolic mirror. The secondary optics consists of a parallel plate collimator of 0.27° acceptance and a Soller slit of 0.04 rad aperture. The measured X-ray results correspond to an average sample area of about 20×20 mm^2. The glancing angle between the incident X-ray beam and the sample surface was set to be 0.255°, i.e., close to the critical angle. Raman spectra were measured by micro-Raman spectroscopy (Renishaw, RM2000) in a backscattering configuration, with a 50 × optical microscope objective. The laser beam was provided by an argon ion laser with a wavelength of 514.4 nm. The photoluminescence (PL) of the samples was studied at room temperature using a 460 nm laser as the excitation source.

3. Results and discussion

3.1. X-ray diffraction

One method of determining the size of crystal grain is through X-ray diffraction (XRD) measurement. By analysing the Bragg diffraction peaks in the XRD spectra, average grain size can be calculated using the Scherrer equation [6]

$$g=\frac{K\lambda}{\Delta(2\theta)\cos\theta} \quad (1)$$

where $\lambda=0.154$ nm is the wavelength of the X-rays, θ is the Bragg diffraction angle at a peak position, $\Delta(2\theta)$ is the full-width at half-maximum (FWHM) of the corresponding peak and K ($=0.9$) is a correction factor. The average diameter of the Si nanocrystals can be calculated by $g'=4/3\,g$, if a spherical shape is assumed [7]. From the XRD data obtained in measurement, four peaks are present at around 21.0°, 28.4°, 47.5° and 56.5°. The first broad peak ($2\theta=21.0°$) is attributed to amorphous SiO_2. The remaining peaks ($2\theta=28.4°$, 47.5° and 56.5°) are resulted from the Bragg peaks of Si (1 1 1), (2 2 0) and (3 1 1). The average Si nanocrystal sizes estimated by Eq. (1) from Si (1 1 1) peaks are summarized in Table 1(a)–(c). The data in the "Difference" column denotes the discrepancy between the actual grain size measured by XRD and the deposition thickness of the SRO layer. A positive value suggests the grain size is larger than the SRO thickness, while a negative value indicates the opposite.

It can be clearly observed from the data that annealing processes with a shorter duration, such as the RTA and "Furnace Short", tend to yield smaller sized nanocrystals. On the other hand, a longer annealing ("Furnace Long") results in larger quantum dots, whose diameter could in some cases exceed the as-deposited thickness of the SRO layer. The XRD data also suggests that a prolonged anneal in conventional furnace results in a higher portion of crystalline phase and generally a larger grain size, as shown in Fig. 2(a). A larger SRO thickness has similar effects (Fig. 2(b)). These results offer slightly different aspects of how variations in structural and annealing length impact the crystallinity and quantum dot size, compared to some other